Modeling Backhaul Deployment Costs in Heterogeneous Radio Access Networks using Spatial Point Processes

Invited Paper

Vinay Suryaprakash and Gerhard P. Fettweis
Vodafone Chair Mobile Communications Systems, TU Dresden, Germany
(vinay.suryaprakash, gerhard.fettweis)@ifn.et.tu-dresden.de

***Abstract*—Future mobile networks are forecast as being increasingly heterogeneous and dense. An aspect crucial to managing such networks is the existence of a flexible and effective backhaul infrastructure. Since backhaul infrastructure is essential, it becomes important to analyze the cost of its implementation. This paper aims to realize a framework to estimate deployment costs in a network which consists of users, two types of base stations, and backhaul nodes that could either be microwave or fiber optic backhaul nodes. The main contribution of this work is the derivation of a framework using spatial point processes that helps estimate the cost of deploying a backhaul node based on the number of users and base stations connected to it. The framework, along with assumptions of typical costs of various network components, is utilized to examine whether there exist an optimal number of backhaul nodes that can minimize the overall deployment cost of a network while catering to a given number of users in the area.**

I. Introduction

An upsurge in the number of mobile Internet users and machine to machine applications has lead to high traffic volumes and dense networks (i.e., heterogeneous networks). A salient aspect in managing these networks efficiently and cost effectively, as presented in [1], is the existence of a sound and flexible backhaul infrastructure. These (dense) networks accompanied by backhaul infrastructure correspond to an increase in the capital invested during their deployment, as shown in [2] and [3]. Hence, it becomes important to be able to estimate the cost of deploying such networks. Works such as [4]–[6] analyze deployment costs of heterogeneous networks, but do so from a more cursory point of view, where they collect data from other sources and estimate deployment costs. However, to the best knowledge of the authors, there have been no efforts to establish a foundation upon which further analysis and optimization of the deployment cost of a heterogeneous network with backhaul infrastructure can be carried out.

Baccelli and Zuyev established such a framework for fixed line telecommunication networks using stationary Poisson processes in [7]. Similarly, this paper presents a method of computing the deployment cost of a network consisting of users, two types of base stations (i.e., macro and micro base stations), and backhaul nodes (or remote network concentrators). The backhaul nodes employ two popular technologies, namely, microwave backhaul and fiber optic backhaul. Influenced by [7], we assume the network consists of 3 layers, each comprising a particular network component (as illustrated in Fig. 1). The users form the bottommost layer, while base stations are on the middle layer, and backhaul nodes are on the topmost layer. The users, base stations, and backhaul nodes are modeled by a stationary Poisson process, a stationary Poisson cluster process, and a stationary mixed Poisson process, respectively. The point processes used to model each layer of the network are defined later on (in Section II). There are three main types of costs which are considered to contribute to the deployment cost, i.e., *equipment cost*, *capacity cost*, and *infrastructure cost*. Unlike equipment costs, the capacity and infrastructure costs are functions of the distance between any two devices, each of which is on a different layer.

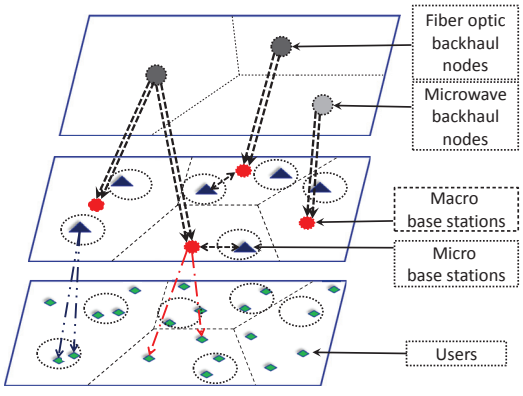

Fig. 1. Illustration of the model considered with users, base stations, and backhaul nodes.

The main result of this work is the derivation of an expression for the total cost of deploying a network[1] which is used to observe fluctuations in the network's deployment cost. Though not proven theoretically, numerical evaluations in this paper also show that there exist a small range of backhaul intensities

[1]Note: The term "network", in this paper, implies a heterogeneous network with backhaul.

978-3-901882-63-0/2014 - Copyright is with IFIP

that can minimize deployment costs for a given number of users in the area. The existence of a range of backhaul intensities that minimize deployment costs for a particular user intensity is surmised from the bowl shaped surfaces that are obtained when figures of variations in deployment costs with increasing backhaul and base station intensities are plotted.

This paper is organized as follows. Section II provides the network model, i.e., a description of the point processes used to model each network component as well as the types of costs that constitute deployment costs. Section III contains the expression for the total deployment cost, whose derivation is detailed in Appendix A. Section IV lists the parameter values assumed to calculate the deployment cost (using the expression derived) along with reasons for the respective assumptions. It also contains Subsection IV-A, which examines variations in deployment costs as a certain subset of parameter values are increased, while the others are kept constant.

II. System Model

This work, inspired by the model in [7] and extending upon our previous work in [8], uses a network model consisting of 3 layers where each layer is independent of the other. The lowest layer consists of users represented by a stationary Poisson process $\Phi_0 \subset \mathbb{R}^2$ with intensity $\lambda_0 > 0$. Both fiber optic and microwave backhaul nodes which belong to the topmost layer are modeled using a stationary mixed Poisson process (see [9]) $\Phi_2 \subset \mathbb{R}^2$ with a randomized intensity function X having a two-point distribution

$$\mathbb{P}\left(X = \lambda_{\text{2MW}}\right) = p, \quad \mathbb{P}\left(X = \lambda_{\text{2OF}}\right) = 1 - p, \quad 0 < p < 1,$$

where p is the probability of having a microwave backhaul and $(1-p)$ is the probability of having a fiber optic backhaul. Hence, the intensity of Φ_2 is

$$\lambda_2 = p\lambda_{\text{2MW}} + (1-p)\lambda_{\text{2OF}},$$

where $\lambda_{\text{2MW}} > 0$ is the intensity of the microwave backhaul and $\lambda_{\text{2OF}} > 0$ is the intensity of the fiber optic backhaul. The middle layer consists of base stations (macro and micro base stations) represented by a stationary Poisson cluster process $\Phi_1 \subset \mathbb{R}^2$ consisting of two parts: cluster centers representing macro base stations and cluster members representing micro base stations. The cluster centers are modeled by a stationary Poisson point process $\Phi_{1c} \subset \mathbb{R}^2$ with intensity $\lambda_{1c} > 0$, and conditioned on Φ_{1c}, the cluster members are modeled by an inhomogeneous Poisson point process $\Phi_{1m} \subset \mathbb{R}^2$ with intensity function

$$\rho(y) = \lambda_{1m} \sum_{x \in \Phi_{1c}} f(y - x), \; y \in \mathbb{R}^2,$$

where $\lambda_{1m} > 0$ is the expected number of cluster members around each cluster center and $f(\cdot)$ is a continuous density function which describes how a cluster member (micro base station) is distributed around a cluster center (macro base station). Note that the cluster intensity and the normalized kernel bandwidth[2] are equal and fixed. Hence, Φ_{1m} is a shot noise Cox process (see [10]) and can also be seen as a Neyman-Scott cluster process (see [11]). This implies Φ_{1m}, when not conditioned on Φ_{1c}, is stationary with intensity $\lambda_{1c}\lambda_{1m}$. Thus, the superposition $\Phi_1 = \Phi_{1c} \cup \Phi_{1m}$ forms a stationary Poisson cluster process with intensity $\lambda_1 = \lambda_{1c}(1+\lambda_{1m})$. The network model can be visualized as shown in Fig. 1. It is important to note that this figure is merely an illustration and does not represent actual realizations of the point processes. Another important assumption is that only connections between adjacent layers are allowed, i.e., there is no direct communication between the backhaul layer and the user layer. This paper also does not explicitly consider costs incurred while connecting backhaul nodes to each other via a mesh network, etc.

An important factor that determines the final cost is the number of users that the network needs to cater to and the number of users that are connected to a given network component. The number of users (or the number of points of Φ_0) that are connected to a given point x in layer Φ_i for $i \geq 1$. This is denoted by $\mathcal{N}_x$ and gives the total number of points in a subtree (as seen in Fig.1). The Voronoi tessellation (see [12]) determines which points of the lower layer are connected to a particular point in the upper layer. In general, the cell centered at a point x belonging to process Φ_i is denoted by $V_x(\Phi_i)$. This structure used in the following sections to estimate the cost of deploying a node in the backhaul layer. However, as shown in [8], defining cell areas for associating users with their respective base stations can also be based on a Signal-to-Interference-plus-Noise (SINR) tessellation which is different from the Voronoi tessellation. In this case, the cell associated with $x \in \Phi_1$ determines the area covered by the base station at x and is given by

$$\mathcal{C}_{x,\Phi_1} = \left\{ z \in \mathbb{R}^2 : \text{SINR}_z \geq T \right\},$$

where T is the threshold and SINR_z is the SINR at point z. A cell of this SINR based tessellation is commonly known, in the wireless engineering community, as a Voronoi cell (see [13] for more information). This definition can then be used to derive expressions for probability of coverage and spectral efficiency which are functions of the user and base station intensities. Hence, the base station intensities required to meet the probability of coverage and spectral efficiency constraints, for a given user intensity, can be calculated quite easily. This can then be used as a factor that influences the deployment cost of the network.

III. Cost Modeling

Since we focus on estimating capital expenditure or deployment cost, typical costs incurred by the service provider can broadly be classified into equipment cost, capacity cost, and infrastructure cost. The *equipment cost* C_i represents the cost of a device deployed in a particular layer i. We assume that users buy their handset, and hence, the cost (to

[2]Kernel bandwidth defines the spread of the cluster points around the parent points and should not be confused with "bandwidth" as defined in communications engineering.

the service provider) $C_0 = 0$. The equipment cost C_1 is the cost of deploying a typical base station cluster consisting of one macro base station and λ_{1m} micro base stations. The equipment cost of a typical backhaul node is C_2 which is a linear combination of $C_{2\text{MW}}$ and $C_{2\text{OF}}$, where $C_{2\text{MW}}$ and $C_{2\text{OF}}$ are the equipment costs of a microwave backhaul device and a fiber optic backhaul device, respectively. The equipment costs of base stations and backhaul nodes can be written as

$$C_1 = \frac{C_{\text{macro}} + \lambda_{1m} C_{\text{micro}}}{(1+\lambda_{1m})},$$
$$C_2 = p\lambda_{2\text{MW}} C_{\text{MW}} + (1-p)\lambda_{2\text{OF}} C_{\text{OF}},$$

where C_{macro} and C_{micro} are the equipment costs of a macro base station and a micro base station, respectively. Note that the cost C_1 is the cost of deploying a single cluster consisting of one parent (macro base station) and an average of λ_{1m} cluster members (micro base stations). Hence, the equipment cost of the (entire) base station layer is

$$\lambda_1 C_1 = \lambda_{1c} C_{\text{macro}} + \lambda_{1c}\lambda_{1m} C_{\text{micro}}.$$

Since all point processes in our model are stationary, for mathematical simplicity, a point under consideration in the higher layer is assumed to be at the origin o. Then, the *capacity cost* is the cost of connecting a device at point x in layer i to another device at point o in layer $i+1$ for a given capacity requirement. This cost is considered to be of the form $A_{i,i+1}\, g(\|x\|)$, where $A_{i,i+1} > 0$ is the base cost to achieve a certain capacity (or data rate) and $g(\|x\|)$ is a function of the distance $\|x\|$ which determines how the base cost scales with distance. For simplicity, $g(\|x\|)$ can be considered to be in power law form given by $g(\|x\|) = \|x\|^{\beta_{i,i+1}}$ where $\|x\|$ is the distance between the points $o \in \Phi_{i+1}$ and $x \in \Phi_i$, and $\beta_{i,i+1} > 0$ is the exponent based on which the cost increases. E.g., if $\beta_{i,i+1} = 1$, $A_{i,i+1}\, g(\|x\|) = A_{i,i+1}\, \|x\|$ which implies that the capacity cost increases linearly with distance. Similarly, the *infrastructure cost* is the physical cost (or expense incurred) to ensure that a point x of layer i and the point o in layer $i+1$ are connected. It is considered to be of the form $B_{i,i+1}\, h(\|x\|)$, where $B_{i,i+1} > 0$ is a quantity similar to $A_{i,i+1}$ (defined as the base cost for a particular type of installation) and $h(\|x\|)$ is a function of the distance $\|x\|$ between the two points under consideration. Once again, for ease of computation, $h(\|x\|)$ is taken to be $\|x\|^{\theta_{i,i+1}}$ where $\theta_{i,i+1} > 0$ determines how fast the base infrastructure cost increases with distance. Though the definitions of capacity and infrastructure costs are similar, the reason for considering them separately is as follows. Infrastructure cost is the cost incurred while laying the cable or installing microwave equipment which increases with the distance between the two points to be connected (due to labor charges, etc.). Furthermore, each technology has the ability to deliver a given data rate (with minimal losses) up to a particular distance for a fixed cost. Now, if the data rate desired is more than what a single installation of a particular technology can provide, it requires more than one installation of the same technology. Since additional installations can use the same physical route (e.g., cabling along the same path) as the initial installation, there is no (or negligible) infrastructure cost but there is added expenditure to meet capacity requirements, such as upgrading certain components, spectrum costs (in the case of a microwave backhaul), etc. Hence, the need for a separate cost category which we term as the capacity cost.

Let $\mathcal{C}_{\Phi_2}$ be the expected cost of deploying a device in the backhaul layer. Then, we have the following theorem.

Theorem 1. *In a 3-layer model that uses power law functions to describe capacity and infrastructure costs, the expected cost of deploying a device in the backhaul layer is given by*

$$\mathcal{C}_{\Phi_2} = \frac{\lambda_1}{\lambda_2}\Bigg[C_1 + \frac{\lambda_0}{\lambda_1}\Psi_1\big(A_{1,2}, \beta_{1,2}, \lambda_{2MW}, \lambda_{2OF}, p\big) + \Psi_2\big(B_{1,2}, \theta_{1,2}, \lambda_{2MW}, \lambda_{2OF}, p\big) + \frac{\lambda_0}{\lambda_1}\Big[\Psi_3\big(A_{0,1}, \beta_{0,1}, \lambda_{1c}, \lambda_{1m}, f(\cdot), \sigma^2\big) + \Psi_4\big(B_{0,1}, \theta_{0,1}, \lambda_{1c}, \lambda_{1m}, f(\cdot), \sigma^2\big)\Big]\Bigg] \tag{1}$$

where $\Psi_1(\cdot)$,$\Psi_2(\cdot)$,$\Psi_3(\cdot)$, and $\Psi_4(\cdot)$ are given by the equations (6), (7), (13), and (14), respectively.

The proof is derived in Appendix A. Therefore, the total cost of such a network is given by

$$C_{\text{TOT}} = C_2 + \lambda_2 \mathcal{C}_{\Phi_2}, \tag{2}$$

where C_2,as defined earlier, is the equipment cost of the backhaul layer. Note that though expressions for $\Psi_3(\cdot)$ and $\Psi_4(\cdot)$ are not closed form expressions like those for $\Psi_1(\cdot)$ and $\Psi_2(\cdot)$, solving them numerically is quite easy.

IV. Utility of the Framework

This work uses [14], [15], and [16] as the basis for all cost values. The equipment costs are tabulated in Table I, while Table II lists the values of the exponents, and Table III lists the base infrastructure and capacity costs used in this paper. It is important to note that the sources, [14]–[16], contain a whole

TABLE I
Table of Equipment Costs

Type of Cost	Value (in $)
C_{macro}	50000
C_{micro}	20000
C_{MW}	50000
C_{OF}	100000

TABLE II
Table of Exponents

Exponents	Type of backhaul	
	Microwave	Optic Fiber
$\beta_{0,1}$	4	4
$\beta_{1,2}$	2	1
$\theta_{0,1}$	2	2
$\theta_{1,2}$	2	1

TABLE III
TABLE OF BASE COSTS

Type of Cost (in $)	Values	Type of Back-haul	
		Microwave	Optic Fiber
Capacity Cost	$A_{0,1}$	5000	5000
	$A_{1,2}$	9000	5000
Infrastructure Cost	$B_{0,1}$	10000	10000
	$B_{1,2}$	20000	100000

range of values for each device and we consider the average value of each type. These sources also provide the cost of a particular device and the range (in terms of radial distance) it can cover from which, the values of the exponents listed in Table II have been extrapolated. The reasons for the choice of values in Table II are as follows.

- The capacity cost between a user and base station is assumed to scale with distance according to the pathloss exponent. We assume a dense urban scenario for which the pathloss is approximately 4 (see [17]). Therefore, $\beta_{0,1} = 4$.
- Data in [16] indicates that the capacity cost for a fiber optic backhaul scales linearly with distance, i.e., farther the distance a given capacity has to be provided to, greater would be the cost. Therefore, $\beta_{1,2} = 1$.
- In case of a microwave backhaul, extrapolation from data collected in [15] shows that the capacity cost between a base station and a backhaul node scales quadratically with distance. Therefore, $\beta_{1,2} = 2$.
- Comparing the costs of base stations and their respective coverage areas in [14], we infer that the infrastructure cost between a user and a base station scales quadratically with distance. Hence, $\theta_{0,1} = 2$ irrespective of the backhaul technology chosen.
- From [16], we assume that the infrastructure cost for a fiber backhaul scales linearly with distance. Hence, $\theta_{1,2} = 1$.
- As in the case of the capacity cost for a microwave backhaul, from [15], it can be concluded that infrastructure cost increases quadratically with distance. Therefore, $\theta_{1,2} = 2$.

It is also important to note that these values merely serve an illustrative purpose in highlighting the usefulness of the expression derived and the accuracy of the values is not our primary concern. Another salient parameter in this framework is the user density λ_0, the value for which can be found based on [17]. In [17], Auer et al. state that the maximum rate density for a dense urban area is 120 Mbps/km^2. Therefore, considering an average user demand of 1 Mbps for illustrative purposes, results in a user intensity $\lambda_0 = 120/\text{km}^2$. The cluster distribution, $f(\cdot)$, also plays a significant role and we assume $f(\cdot)$ to be a radially symmetric zero-mean Gaussian density with variance $\sigma^2 = 0.5$ (except in Fig. 7 and Fig. 8). A rather large variance is chosen to ensure that the micro base stations are fairly widely spread out around the macro base station. Thereby, reflecting a relatively realistic deployment scenario. The probability of occurrence of either type of backhaul infrastructure is assumed to be equally likely, i.e., $p = 0.5$. Using all of the above values in equation (1) results in the figures in Subsection IV-A.

A. Examination of the Figures

The expression in equation (1) has a lot of parameters which can be varied. The tables I – III assign values for most of the costs except for macro and micro base station intensities, intensities of the microwave and fiber optic backhaul, and the cluster variance. It is important to note that, since we deploy base stations in clusters (i.e., one macro base station with λ_{1m} micro base stations on average), increasing the macro base station intensity is equivalent to increasing the overall base station intensity. An aspect that is immediately obvious from the figures (in this section) is that the deployment cost of the network can be computed quite easily, for any given set of cost and parameter values. A closer examination of the figures reveals the following.

Fig. 2 shows variations in the total deployment cost when all other values except the microwave backhaul intensity and the macro base station intensity are kept fixed. The cost "surface" obtained takes a sort of a bowl shape. The shape of the surface highlights the existence of a small range of microwave backhaul intensity values that can minimize the network's deployment cost. A similar observation can be made in Fig. 3 where the bowl shaped surface is obtained by varying the fiber optic backhaul intensity and the macro base station intensity, while keeping all the other parameters fixed. The reason for the bowl shaped curves in Fig. 2 and Fig. 3 can be explained as follows. At very low base station and backhaul intensities (though the intensity of one of the backhaul technologies is kept fixed), the distance between devices in the backhaul layer and the base station layer tend to be quite large. This increases the capacity and infrastructure costs, and hence, results in very high deployment costs. As the intensities of base stations and one of the backhaul technologies in the backhaul layer are increased, the distance between devices in the two layers decreases leading to lower deployment costs. However, above a certain base station and backhaul intensity, the equipment cost begins to play a more decisive role due to the sheer number of devices. This ultimately leads to an increase in the deployment cost of the network.

Fig. 4 illustrates deployment cost when both microwave and fiber optic backhaul intensities are varied, with all other parameters and costs kept constant. As in Fig. 2 and Fig. 3, deployment costs are high when the intensities are low due to high capacity and infrastructure costs caused by large distances between devices in the two layers. The deployment cost decreases as the intensity of the backhaul technologies increase and sort of plateaus beyond a particular value. The plateauing effect is because the base station intensity as well as the other parameters are fixed. This plateauing effect, however, is only illusory as seen in Fig. 5, which depicts much higher (and rather unrealistic) intensities for both types of backhaul technologies and base stations. Fig. 5 clearly illustrates that a bowl shaped surface is obtained in this case as well. The

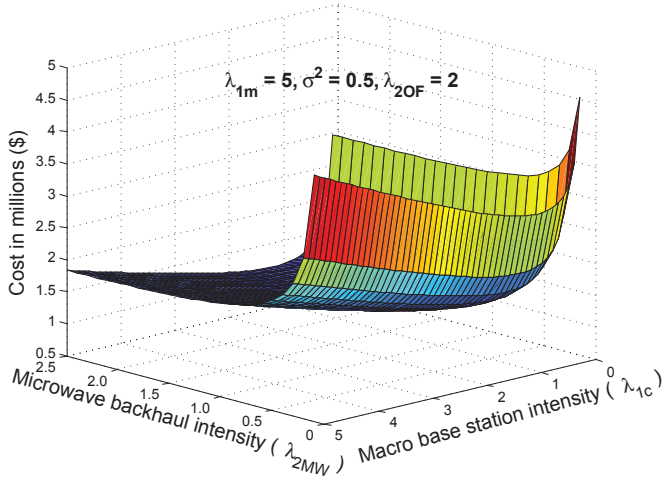

Fig. 2. Variation of deployment cost of a network with increasing macro base station and microwave backhaul intensities.

existence of a small range of backhaul intensities that can minimize network costs is further corroborated by Fig. 6 which is a contour plot of Fig. 5. It should be noted that contour plots for the other figures have not been shown because the equipment costs considered in this work are rather low and, for intensities of practical interest considered in the figures, they do not illustrate the minimal cost region as clearly as in Fig. 6. Another important reason for the omission is the brevity of the paper.

The variation in deployment cost corresponding to an increase in the cluster variance and the microwave backhaul intensity (while all other cost and parameter values are fixed) is shown in Fig. 7. This figure illustrates that deployment costs are extremely high at low microwave backhaul intensities due to high infrastructure and capacity costs, which in turn are due to large distances between devices in the backhaul and base station layers. Initially, the deployment cost decreases quite rapidly for a small increase in backhaul intensity. After a particular backhaul intensity value, the decrease in deployment cost ultimately slows and starts to increase very gradually as

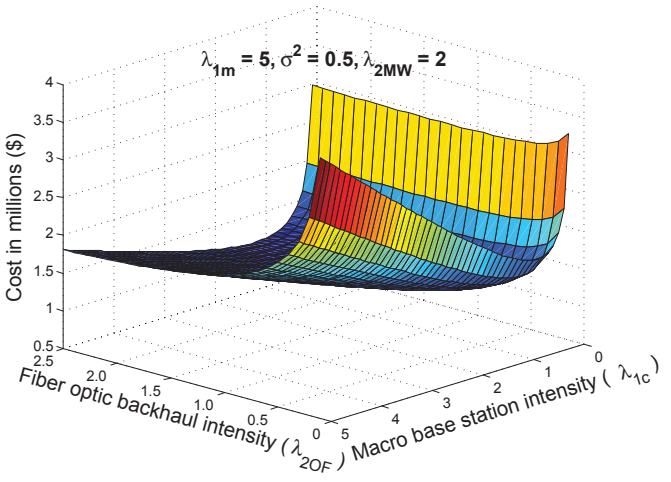

Fig. 3. Variation of deployment cost of a network with increasing macro base station and fiber optic backhaul intensities.

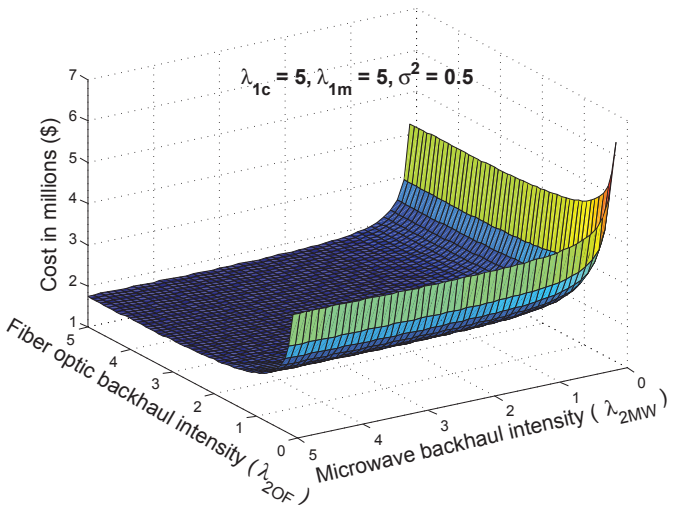

Fig. 4. Variation of deployment cost of a network with increasing macro base station and microwave backhaul intensities.

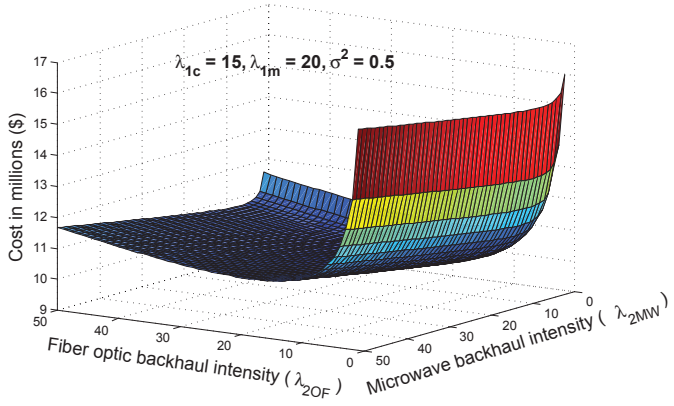

Fig. 5. Variation of deployment cost of a network with very large fiber optic backhaul and microwave backhaul intensities.

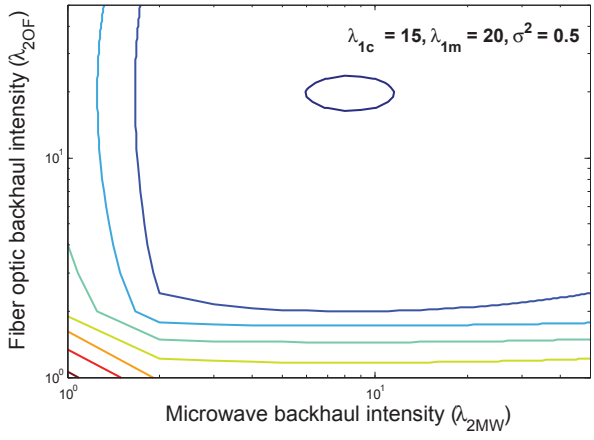

Fig. 6. Variation of deployment cost of a network with very large fiber optic backhaul and microwave backhaul intensities as a contour plot.

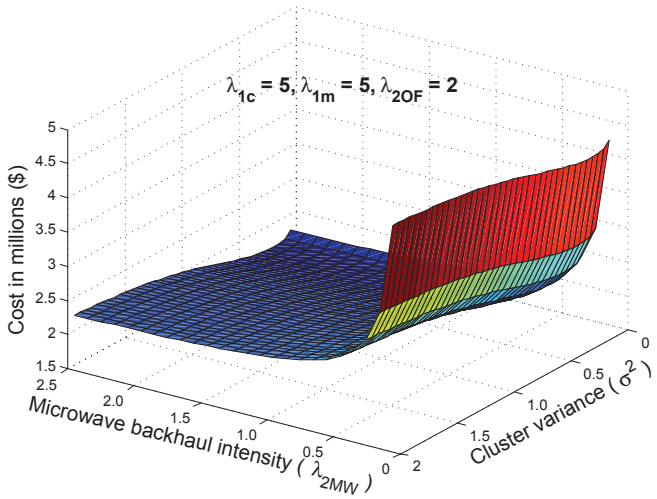

Fig. 7. Variation of deployment cost of a network with increasing microwave backhaul intensity and cluster variance.

equipment costs start to play a more significant role. However, it is important to note that for a given microwave backhaul density, the deployment costs increase as the cluster variance increases and this behavior can be explained as follows. An increase in cluster variance implies that the micro base stations are more widely spread out around the macro base station, which results in an increase in the capacity and infrastructure costs, and consequently, in a higher deployment cost. Fig. 8 shows that a similar behavior is seen when the fiber optic backhaul intensity and the cluster variance are increased. The reasons for the surface obtained in Fig. 8 are the same as those stated for Fig. 7.

V. Summary

This paper details a method of modeling heterogeneous networks along with their backhaul infrastructure using spatial point processes. The main contribution of this work is the derivation of an expression using a point process model that allows us to compute the total cost of deploying such a network when there are a given number of users in the area that need to be catered to. The expression establishes a relationship between the intensities of different network components (users, macro and micro base stations, and microwave & fiber optic backhaul nodes), the base costs (capacity, equipment, and infrastructure costs), and the manner in which these costs scale with distance between two different network components. This framework is then used to compute the deployment cost of a network when the intensities of its components increase. Observing these figures indicates that there exists a backhaul intensity (or a small range of backhaul intensities) that can minimize deployment costs while catering to all base stations and their respective users.

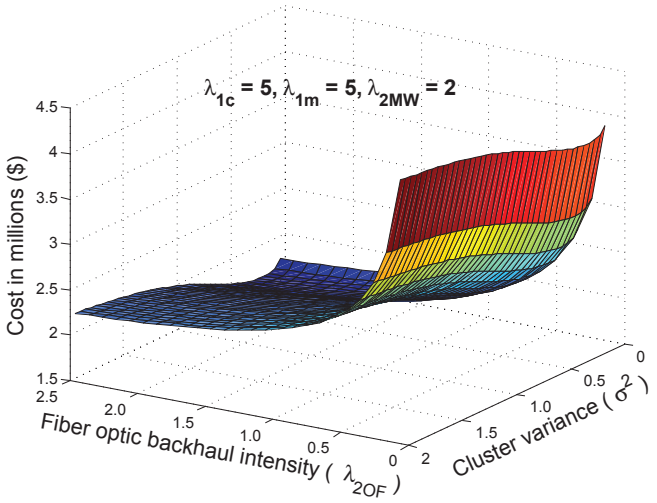

Fig. 8. Variation of deployment cost of a network with increasing fiber optic backhaul intensity and cluster variance.

Acknowledgment

The research leading to these results has received funding from the European Union Seventh Framework Programme (FP7/2007-2013) under grant agreement no. 317941 – project iJOIN.

Appendix A
Proof of Theorem

Proof: The aggregate average cost of the back-haul node layer, $\mathcal{C}_{\Phi_2}$, for a 3-layer model can be defined as

$$\mathcal{C}_{\Phi_2} = \mathbb{E}^o_{\Phi_2}\Bigg[\sum_{y\in\Phi_1\cap V_o(\Phi_2)}\Big\{C_1+\mathcal{N}_y A_{1,2}\|y\|^{\beta_{1,2}}+B_{1,2}\|y\|^{\theta_{1,2}}+\sum_{x\in\Phi_0\cap V_y(\Phi_1)}\left(A_{0,1}\|x-y\|^{\beta_{0,1}}+B_{0,1}\|x-y\|^{\theta_{0,1}}\right)\Big\}\Bigg],$$

where $\mathbb{E}^o_{\Phi_2}[\cdot]$ is the expectation over the Palm distribution of the process Φ_2. Separating the terms after using the exchange formula of Neveu (see [18]) results in

$$\mathcal{C}_{\Phi_2} = \frac{\lambda_1}{\lambda_2}\Bigg[C_1+\mathbb{E}^o_{\Phi_1}\left[\mathcal{N}_o A_{1,2}\|z_o\|^{\beta_{1,2}}\right]+\mathbb{E}^o_{\Phi_1}\left[B_{1,2}\|z_o\|^{\theta_{1,2}}\right]+\mathbb{E}^o_{\Phi_1}\Bigg[\sum_{x\in\Phi_0\cap V_o(\Phi_1)}\left(A_{0,1}\|x\|^{\beta_{0,1}}+B_{0,1}\|x\|^{\theta_{0,1}}\right)\Bigg]\Bigg], \quad (3)$$

where the point of observation is shifted to the origin 'o' and $\|z_o\|$ is the effective distance between a point in the backhaul layer and a point in the base station layer.

Since the point processes in each layer are independent of the others, we can write the second term of the RHS of equation (3) as $\mathbb{E}^o_{\Phi_1}[\mathcal{N}_o]\,\mathbb{E}^o_{\Phi_1}\left[A_{1,2}\|z_o\|^{\beta_{1,2}}\right]$. From [13], we get $\mathbb{E}^o_{\Phi_1}[\mathcal{N}_o]=\frac{\lambda_0}{\lambda_1}$. The terms $\mathbb{E}^o_{\Phi_1}\left[A_{1,2}\|z_o\|^{\beta_{1,2}}\right]$ and

$\mathbb{E}^o_{\Phi_1}\left[B_{1,2}\|z_o\|^{\theta_{1,2}}\right]$ can (both) be simplified as shown below.

$$\begin{aligned}\mathbb{E}^o_{\Phi_1}&\left[A_{1,2}\|z_o\|^{\beta_{1,2}}\right]\\ &\overset{(a)}{=} A_{1,2}\mathbb{E}\int_{\mathbb{R}^2}\|a\|^{\beta_{1,2}}\mathbf{1}\left(\Phi_2\left(b(o,\|a\|)=0\right)\right)\Phi_2(\mathrm{d}a)\\ &\overset{(b)}{=} A_{1,2}\,\lambda_2\int_{\mathbb{R}^2}\|a\|^{\beta_{1,2}}\mathbb{P}^o_2\left(b(-a,\|a\|)\right)\mathrm{d}a \qquad (4)\end{aligned}$$

Here, equality (a) is (once again) due to independence of the processes and $\Phi_2(\cdot)$ is the stationary random measure on $\mathbb{R}^2$. The equality (b) is due to the Refined Campbell theorem (see [18]) where $\mathbb{P}^o_2(\cdot)$ is the Palm distribution with respect to the point process Φ_2, which is defined as shown in equation (5) (see [9]). After substituting equation (5) in equation (4) and integrating, we obtain equation (6). Similarly, the third term of the RHS of equation (3) can be written as equation (7). Finally, the Palm expectation of the last term of the RHS of equation (3) can be simplified by using the exchange formula of Neveu once again. This results in

$$\begin{aligned}\mathbb{E}^o_{\Phi_1}&\left[\sum_{x\in\Phi_0\cap V_o(\Phi_1)}\left(A_{0,1}\|x\|^{\beta_{0,1}}+B_{0,1}\|x\|^{\theta_{0,1}}\right)\right]=\\ &\frac{\lambda_0}{\lambda_1}\Big[\mathbb{E}^o_{\Phi_0}\left[A_{0,1}\|a_o\|^{\beta_{0,1}}\right]+\mathbb{E}^o_{\Phi_0}\left[B_{0,1}\|a_o\|^{\theta_{0,1}}\right]\Big], \qquad (10)\end{aligned}$$

where $\|a_o\|$ is the effective distance between the base station at o and a user (under consideration). Then, following up with the use of the Refined Campbell theorem (see [18]) similar to equation (4), we obtain

$$\mathbb{E}^o_{\Phi_0}\left[A_{0,1}\|z_o\|^{\beta_{0,1}}\right]=A_{0,1}\,\lambda_1\int_{\mathbb{R}^2}\|a\|^{\beta_{0,1}}\mathbb{P}^o_1\left(b(-a,\|a\|)\right)\mathrm{d}a \qquad (11)$$

for the first term on the RHS of equation (10). The Palm distribution $\mathbb{P}^o_1(\cdot)$ can be found by means of the J-function (see [19]) and the "empty space function", F (see [10]). The Palm distribution is

$$\mathbb{P}^o_1(b(o,R))=1-\left[1-F_{\Phi_1}(R)\right]J_{\Phi_1}(R), \qquad (12)$$

where R is the random distance from o to the nearest point in Φ_1 (due to the stationarity of Φ_1). Note that for a realization r of the distance R, the Palm distribution can be obtained by taking the derivative of equation (12) with respect to r. The J-function of $J_{\Phi_1}(R)$, is given by

$$\begin{aligned}J_{\Phi_1}(R)&=J_{\Phi_{1c}\cup\Phi_{1m}}(R)\\ &=\frac{\lambda_{1c}}{\lambda_{1c}+\lambda_{1c}\lambda_{1m}}J_{\Phi_{1c}}(R)+\frac{\lambda_{1c}\lambda_{1m}}{\lambda_{1c}+\lambda_{1c}\lambda_{1m}}J_{\Phi_{1m}}(R),\end{aligned}$$

since the processes Φ_{1c} and Φ_{1m} are independent stationary point processes (see [19] and [20] for details). As shown in [19], since Φ_{1c} is a stationary Poisson process, $J_{\Phi_{1c}}(R)=1$ and $J_{\Phi_{1m}}(R)$ can be derived as

$$J_{\Phi_{1m}}(R)=\int_{\mathbb{R}^2}f(x)\exp\Big(-\int_{\|y\|\le R}\lambda_{1m}f(y+x)\mathrm{d}y\Big)\mathrm{d}x,$$

from the general expression for stationary Cox processes provided in [10]. Hence, the J-function can be written as equation (8). Then, recalling that $\left[1-F_{\Phi_1}(R)\right]$ is the *void probability*, we get equation (9) (see [9]). Hence, the Palm distribution can be found by substituting equations (8) and (9) in equation (12). Therefore, recalling that Φ_1 is stationary, for a realization $R=r$, equation (11) becomes

$$\begin{aligned}\Psi_3\big(A_{0,1},\beta_{0,1},\lambda_{1c},\lambda_{1m},f(\cdot),\sigma^2\big)&\equiv\mathbb{E}^o_{\Phi_0}\left[A_{0,1}\|z_o\|^{\beta_{0,1}}\right]\\ &=A_{0,1}\,\lambda_1\int_{\mathbb{R}}r^{\beta_{0,1}}\mathbb{P}^o_1\left(b(o,r)\right)\mathrm{d}r.\end{aligned} \qquad (13)$$

Similarly,

$$\begin{aligned}\Psi_4\big(B_{0,1},\theta_{0,1},\lambda_{1c},\lambda_{1m},f(\cdot),\sigma^2\big)&\equiv\mathbb{E}^o_{\Phi_0}\left[B_{0,1}\|z_o\|^{\theta_{0,1}}\right]\\ &=B_{0,1}\,\lambda_1\int_{\mathbb{R}}r^{\theta_{0,1}}\mathbb{P}^o_1\left(b(o,r)\right)\mathrm{d}r.\end{aligned} \qquad (14)$$

Then, substitute equations (13) and (14) in equation (10). Finally, substituting equations (6), (7), and (10) in equation (3) results in equation (1). It is important to note that though closed form expressions similar to equations (6) and (7) cannot be obtained for equations (13) and (14), they can be solved quite easily using numerical integration. Numerical integration is especially simple if the cluster distribution $f(\cdot)$ is a zero-mean radially symmetric Gaussian density with variance σ^2. ■

REFERENCES

[1] P. Rost, C. Bernardos, A. D. Domenico, M. D. Girolamo, M. Lalam, A. Maeder, D. Sabella, and D. Wübben, "Cloud technologies for flexible 5g radio access networks," *Accepted for publication at in 5G Special Issue of IEEE Communications Magazine*, May 2014. [Online]. Available: http://ieeexplore.ieee.org/xpl/RecentIssue.jsp?punumber=35

[2] International Telecommuncations Union. [Online]. Available: mobithinking.com/mobile-marketing-tools/latest-mobile-stats/a#subscribers

[3] Pacific West Communications Inc. [Online]. Available: http://www.pwc.com/gx/en/communications/publications/we-need-to-talk-about-capex-benchmarking-best-practice-in-telecom-capital-allocation.jhtml

[4] B. Lannoo, M. Kantor, L. Wosinska, K. Casier, J. Van Ooteghem, S. Verbrugge, J. Chen, K. Wajda, and M. Pickavet, "Economic analysis of future access network deployment and operation," in *Transparent Optical Networks, 2009. ICTON '09. 11th International Conference on*, 2009, pp. 1–4.

[5] M. Paolini, "Crucial economics for mobile data backhaul," *White paper, Senzafili Consulting*, 2011. [Online]. Available: http://www.shamwana.co.uk/cbnl/sites/all/files/userfiles/files/CB-002070-DC-LATEST.pdf

[6] H. Claussen, L. T. W. Ho, and L. Samuel, "Financial analysis of a pico-cellular home network deployment," in *Communications, 2007. ICC '07. IEEE International Conference on*, 2007, pp. 5604–5609.

[7] F. Baccelli and S. Zuyev, "Poisson-voronoi spanning trees - with applications to the optimization of communication networks," *Operations Research*, vol. 47, pp. 619–631, 1997.

[8] V. Suryaprakash and G. Fettweis, "An analysis of backhaul costs of radio access networks using stochastic geometry," *Accepted for publication at the International Communications Conference (ICC) 2014 IEEE, Sydney, Australia.*, 2014.

[9] D. Stoyan, W. S.Kendall, and J. Mecke, *Stochastic Geometry and its Applications*. John Wiley and Sons, New York, 1995.

$$\mathbb{P}_2^o\left(b(-a,\|a\|)\right) = \frac{1}{\lambda_2}\left[p\,\lambda_{\text{2MW}}\mathbb{P}_{\text{2MW}}^o\left(b(-a,\|a\|)\right) + (1-p)\lambda_{\text{2OF}}\mathbb{P}_{\text{2OF}}^o\left(b(-a,\|a\|)\right)\right]$$
$$= \frac{1}{\lambda_2}\left[p\,\lambda_{\text{2MW}}\exp\left(-\pi\lambda_{\text{2MW}}\|a\|^2\right) + (1-p)\lambda_{\text{2OF}}\exp\left(-\pi\lambda_{\text{2OF}}\|a\|^2\right)\right] \quad (5)$$

$$\Psi_1\big(A_{1,2},\beta_{1,2},\lambda_{\text{2MW}},\lambda_{\text{2OF}},p\big) \equiv \mathbb{E}_{\Phi_1}^o\left[A_{1,2}\|z_o\|^{\beta_{1,2}}\right] = A_{1,2}\left[\frac{p\,\Gamma(\frac{\beta_{1,2}}{2}+1)}{(\pi\lambda_{\text{2MW}})^{\beta_{1,2}/2}} + \frac{(1-p)\,\Gamma(\frac{\beta_{1,2}}{2}+1)}{(\pi\lambda_{\text{2OF}})^{\beta_{1,2}/2}}\right] \quad (6)$$

$$\Psi_2\big(B_{1,2},\theta_{1,2},\lambda_{\text{2MW}},\lambda_{\text{2OF}},p\big) \equiv \mathbb{E}_{\Phi_1}^o\left[B_{1,2}\|z_o\|^{\theta_{1,2}}\right] = B_{1,2}\left[\frac{p\,\Gamma(\frac{\theta_{1,2}}{2}+1)}{(\pi\lambda_{\text{2MW}})^{\theta_{1,2}/2}} + \frac{(1-p)\,\Gamma(\frac{\theta_{1,2}}{2}+1)}{(\pi\lambda_{\text{2OF}})^{\theta_{1,2}/2}}\right] \quad (7)$$

$$J_{\Phi_1}(R) = \frac{\lambda_{1c}}{\lambda_{1c}+\lambda_{1c}\lambda_{1m}} + \frac{\lambda_{1c}\lambda_{1m}}{\lambda_{1c}+\lambda_{1c}\lambda_{1m}}\left[\int_{\mathbb{R}^2} f(x)\exp\Big(-\int_{\|y\|\le R}\lambda_{1m}f(y+x)\mathrm{d}y\Big)\mathrm{d}x\right]. \quad (8)$$

$$1-F_{\Phi_1}(R) = \exp\left(-\lambda_{1c}\int_{\mathbb{R}^2}\left[1-\mathbf{1}\left(x\notin b(o,R)\right)\exp\Big(-\lambda_{1m}\int_{b(o,R)} f(y-x)\,\mathrm{d}y\Big)\right]\mathrm{d}x\right). \quad (9)$$

[10] J. Møller, "Shot noise Cox processes," *Advances in Applied Probability*, vol. 35, pp. 4–26, 2003.

[11] J. Neyman and E. Scott, "Statistical approach to problems of cosmology," *Journal of the Royal Statistical Society: Series B (Statistical Methodology)*, vol. 20, pp. 1–43, 1958.

[12] J. Møller, *Lectures on Random Voronoi Tessellations*, ser. Lecture Notes in Statistics 87. Springer-Verlag, New York, 1994.

[13] F. Baccelli and B. Blaszczyszyn, "Stochastic Geometry and Wireless Networks Volume 1: THEORY," *Foundations and Trends in Networking*, vol. 3, pp. 249–449, 2009.

[14] K. Johansson, A. Furuskar, P. Karlsson, and J. Zander, "Relation between base station characteristics and cost structure in cellular systems," in *Personal, Indoor and Mobile Radio Communications, 2004. PIMRC 2004. 15th IEEE International Symposium on*, vol. 4, 2004, pp. 2627–2631 Vol.4.

[15] Exalt communications inc. [Online]. Available: http://www.exaltcom.com/Economics-of-Backhaul.aspx

[16] The fiber optic association. [Online]. Available: http://www.thefoa.org

[17] G. Auer, V. Giannini, I. Godor, P. Skillermark, M. Olsson, M. A. Imran, D. Sabella, M. Gonzales, C. Desset, and O. Blume, "Cellular energy efficiency evaluation framework," *Green Wireless Communications and Networks Workshop 2 with VTC*, 2011.

[18] R. Schneider and W. Weil, *Stochastic and Integral Geometry*. Springer-Verlag, 2008.

[19] M. N. M. van Lieshout and A. J. Baddeley, "A Nonparametric Measure Of Spatial Interaction In Point Patterns," *Statistica Neerlandica*, vol. 50, pp. 344 – 361, 1996. [Online]. Available: http://oai.cwi.nl/oai/asset/10665/10665A.pdf

[20] A. J. Baddeley, "Spatial point processes and their applications," in *Stochastic Geometry*, ser. Lecture Notes in Mathematics, W. Weil, Ed. Springer Berlin Heidelberg, 2007, vol. 1892, pp. 1–75. [Online]. Available: http://dx.doi.org/10.1007/978-3-540-38175-4_1